Appendix 2. Analytical methods for U-Pb dating on zircon grains and complementary geochronological results.

1. Operating conditions and instruments settings

Operating conditions and instruments settings are detailed in Supplementary Table 3.

Supplementary Table 3. Operating conditions and instrument settings for U-Pb analyses.

Laboratory and sample preparation	
Laboratory name	*Laboratório de Geoquímica Isotópica, Departamento de Geologia, Universidade Federal de Ouro Preto, Departamento de Geologia*, Ouro Preto, Brazil.
Sample type/mineral	Sandstones and conglomerates/detrital zircon grains.
Sample preparation	Conventional mineral separation: rock crushing, hand panning, removal of the most magnetic minerals fraction with a hand magnet, heavy liquid separation (methylene iodide) and Frantz isodynamic magnetic separator. Frantz settings and were kept below 1.8 A and 10° side-slope (Sircombe and Stern, 2002). Grains were handpicked under binocular microscope. Despite efforts to produce the most representative sampling as possible, potential bias during grain selection is possible in samples containing numerous zircon grains ((Košler et al., 2013). In samples containing a limited number of grains (n < 200), all grains were mounted, limiting such bias. Grains were mounted in an 1 inch resin mount, 1μm polish to finish.
Imaging	Cathodoluminscence imaging by Scanning Electron Microscopy (SEM) using a *JEOL 6510* equipped with a *Centaurus* cathodoluminescence detector by the Laboratorio de Microscopia e Microanalises do DEGEO/EM – Rede de Microscopia a Microanalise de Minas Gerais – FAPEMIG, Universidade Federal de Ouro Preto, Departamento de Geologia, Brazil.
Laser ablation system	
Make, model and type	Photon machine G2 Excimer laser
Ablation cell and volume	Low volume HelEx
Laser wavelength	193 nm
Pulse width	< 4 ns
Fluence	ca. 8 $J.cm^{-2}$
Repetition rate	10 Hz
Spot size	30 μm
Ablation duration	40 seconds
Ablation pit depth	ca. 10 μm pit depth
Sampling mode/pattern	Static single spot ablation
Carrier gas	100% He in the cell, Ar and N2 make-up gas, combined using two Y-piece 50% along the sample transport line to the torch.
Cell carrier gas flow	1.2 $L.min^{-1}$ He
ICP-MS Instrument	
Make, model and type	ThermoFisher Scientific, Element II, SF-ICP-MS

Sample introduction	Ablation aerosol
RF power	1200 W
Make-up gas flow	0.8 $L.min^{-1}$
Detection system	SEM/discrete dynode detector system
Masses measured	202; 204; 206; 207; 208; 238 The ^{235}U signal is calculated from ^{238}U using the ratio $^{235}U/^{238}U = 137.88$.
Integration time per peak	4 ms for each isotope
Total integration time per output data point	0.130 second
IC Dead time	18 ns
Data Processing	
Gas blank	20 seconds
Calibration strategy	Sample bracketing; GJ1 zircon used as primary reference material.
Reference material info	(Jackson et al., 2004)
Data processing package used	Glitter 4.4.3 software (van Achterbergh et al., 2004). Laser induced elemental fractionation correction assumes that reference material and sample behave identically.
Mass discrimination	Corrected by normalization to the primary reference material.
Common-Pb correction. Concentrations and uncertainties	No common-Pb correction applied to the data. Concentrations (U, Pb, Th) uncertainties are ca. 20%
Uncertainty level and propagation	Ages are quoted at 95% confidence level; propagation is by quadratic addition. Reproducibility and age uncertainty of reference material are propagated where appropriate.
Quality control/Validation	Plesovice: weighted $^{206}Pb/^{238}U$ mean age = 338.0 ± 0.7 Ma (n=91; MSWD = 0.32, uncertainty at 2σ level), identical, within uncertainties, to the TIMS $^{206}Pb/^{238}U$ age (337.13 ± 0.37 Ma; Sláma et al., 2008). GJ-1 (used as secondary reference material): weighted $^{206}Pb/^{238}U$ mean age = 600.0 ± 1.5 Ma (n=57; MSWD = 0.24, uncertainty at 2σ level), identical, within uncertainties, to the TIMS $^{207}Pb/^{206}Pb$ age (601.86 ± 0.37 Ma; Jackson et al., 2004; Horstwood et al., 2016). BB: weighted $^{206}Pb/^{238}U$ mean age = 560.9 ± 1.8 Ma (n=31; MSWD = 0.5, uncertainty at 2σ level), identical, within uncertainties, to the TIMS $^{206}Pb/^{238}U$ age (560.0 ± 0.4 Ma; Santos et al., 2017).
Other information	For detailed sample preparation and data selection procedures, see Rossignol et al. (2016).

6

2. Comparison of thermal annealing and chemical abrasion and classic procedures

2.1. Methods

To assess the validity of the thermal annealing and chemical abrasion (TACA) procedure, we implemented a twofold procedure: for each sample, we randomly separated the grains in two subsets of ca. 200 grains each. We dated one subset following a classical procedure (Košler and Sylvester, 2003) by Laser Ablation – Inductively Coupled Plasma – Mass Spectrometry (LA-ICP-MS). We submitted the grains of the other subset to the TACA treatment as described in the methodological section of the manuscript.

Most of the U-Pb analyses performed on untreated grains are discordant but align in a ^{206}Pb-^{238}U – ^{207}Pb-^{235}U diagram, suggesting that these grains are cogenetic. The approach thus consisted in calculating the upper intercept of the unforced discordia passing through the analyses. The upper intercept was calculated taking into account the uncertainty of each individual analysis by weighting the data points proportionally to the inverse square of their uncertainties ("model 1" regression in Isoplot; Ludwig, 2012).

2.2. Results

Cathodoluminescence (CL) images of representative grains from the Carajás Formation are presented in Supplementary Fig. 2.

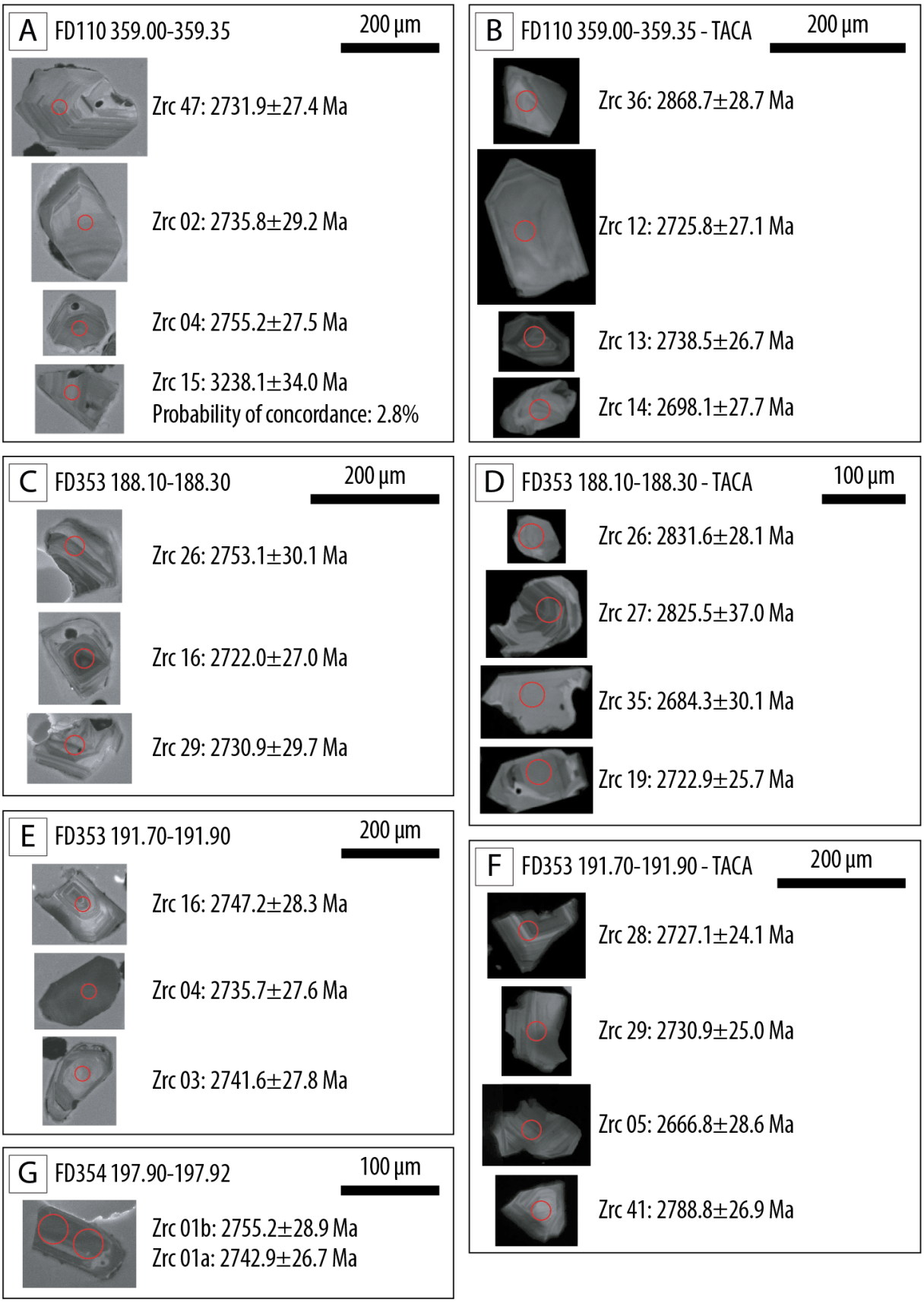

Supplementary Figure 2. Cathodoluminescence images of representative zircon grains of the Carajás Formation.

Left column: zircon grains analyzed following a classical procedure; right column: Thermally Annealed and Chemically Abraded (TACA) grains. Red circles indicate the location of analyses. Uncertainties are given at the 2σ level. (**A, B**) Sample FD110 359.00-359.35. (**C, D**) Sample FD353 188.10-188.30. (**E, F**) Sample FD353 191.70-191.90. (**G**) Sample FD354 197.90-197.92.

FD110 359.00-359.35. About 200 grains from this volcaniclastic basaltic sandstone have been picked up for the TACA procedure and 200 have been kept for the classical procedure. Data obtained from classical analyses display a proportion of concordant data of 65 % (57 out of 88; Supplementary Fig. 3A). All the analyses but two align in a ^{206}Pb-^{238}U – ^{207}Pb-^{235}U diagram, allowing to calculate a date of 2727.8 ± 7.9 Ma (MSWD = 0.63; n = 86; Supplementary Fig. 3A; Supplementary Table 4). Among the two crystals that do not belong to this main population, one result is discordant and the other gives a concordia date of 2951.8 ± 29.6 Ma. This date is similar to those of the rocks forming the basement of the Carajás Basin (Machado et al., 1991; Moreto et al., 2015; Pidgeon et al., 2000) and is interpreted to represent either epicrysts or xenocrysts.

Data obtained from TACA grains show a similar proportion of concordant grains compared to classical analyses (36 out of 57, i.e., 65 % of concordant grains; Supplementary Fig. 3B). Most of the TACA grains are grouped in a cluster of 35 concordant analyses, which gives a concordia date of 2719.6 ± 5.6 Ma (MSWD = 0.47; Supplementary Fig. 3B). This date is identical, within uncertainties, to the upper intercept date calculated from grains dated following a classical procedure.

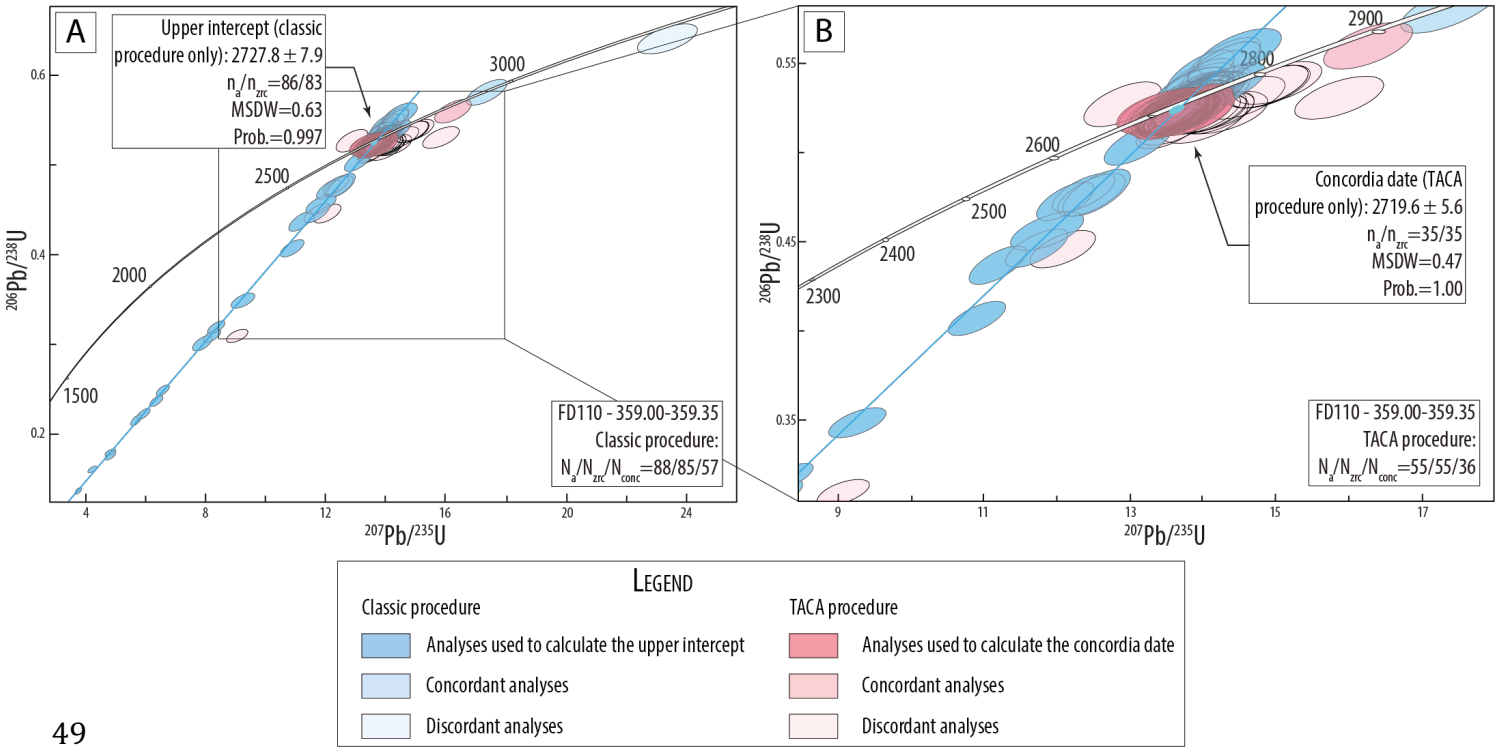

Supplementary Figure 3. Geochronological diagrams for a sample collected in the Carajás Formation to the north of the basin. All the diagrams were generated using Isoplot/Ex 3.00 (Ludwig, 2012). Error ellipses are depicted at the 2σ level. N_a: number of analyses; N_{zrc}: number of zircon grains; N_{conc}: number of concordant zircon grains. MSWD: Mean Square Weighted Deviate (given for both concordance and equivalence when referring to a concordia date); Prob.: probability if fit of the regression (upper intercept date) or probability for concordance and equivalence (concordia date). (**A**) All analyses from both subsets. (**B**) Inset focused on TACA analyses.

FD353 188.10-188.30. This sample yielded a fair amount of zircon grains, among which 100 have been collected for TACA treatment and 150 have been picked up for classic procedure. Data obtained from classical analyses display a rather low proportion of concordant data, with 41% of the analyses being concordant (26 out of 64; Supplementary Fig. 4A). All analyses but one align in a ^{206}Pb-^{238}U – ^{207}Pb-^{235}U diagram, allowing to calculate an upper intercept date of 2723.6 ± 8.5 Ma (MSWD = 0.66; n = 63; Supplementary Fig. 4A; Supplementary Table 4).

Data obtained from TACA grains have a very high proportion of concordant grains (41 out of 42, i.e., 98 % of concordant grains; Supplementary Fig. 4B). The youngest cluster of

concordant grains gives a concordia date of 2732.4 ± 5.2 Ma (MSWD = 0.53; n = 37; Supplementary Fig. 3B). This date is identical, within uncertainties, to the upper intercept age calculated from grains dated following a classical procedure.

FD353 191.70-191.90. Data from classical analyses display a rather low proportion of concordant data, with 41% of the analyses being concordant (34 out of 82; Supplementary Fig. 3C). All the analyses, except one strongly discordant data, can be used to calculate an upper intercept date of 2726.1 ± 8.0 Ma (MSWD = 0.35; n = 81; Supplementary Fig. 4C).

Data obtained from TACA grains have a rather high proportion of concordant grains, with 69 % of concordant analyses (38 out of 55 grains; Supplementary Fig. 3D). The 38 concordant analyses are grouped into a cluster giving a concordia date of 2728.5 ± 5.2 Ma (MSWD = 0.57; Supplementary Fig. 4D). This date is identical, within uncertainties, to the upper intercept age calculated using the classical procedure.

FD354 197.90-197.92. This small sample made up of grey clay interpreted to correspond to diagenetic ashes yielded only three zircon grains, on which four analyses have been performed following a classical procedure. A TACA treatment has not been done on this sample because not enough zircon were available. The grains display well-defined oscillatory zoning (Supplementary Fig. 2) and Th/U ratios ranging between 0.37 and 0.72, typical of magmatic zircon. The four analyses define a discordia line with a rather imprecise upper intercept date of 2743 ± 23 Ma (MSWD = 0.27; Supplementary Fig. 4E). This date is interpreted as the maximum depositional age for this sample.

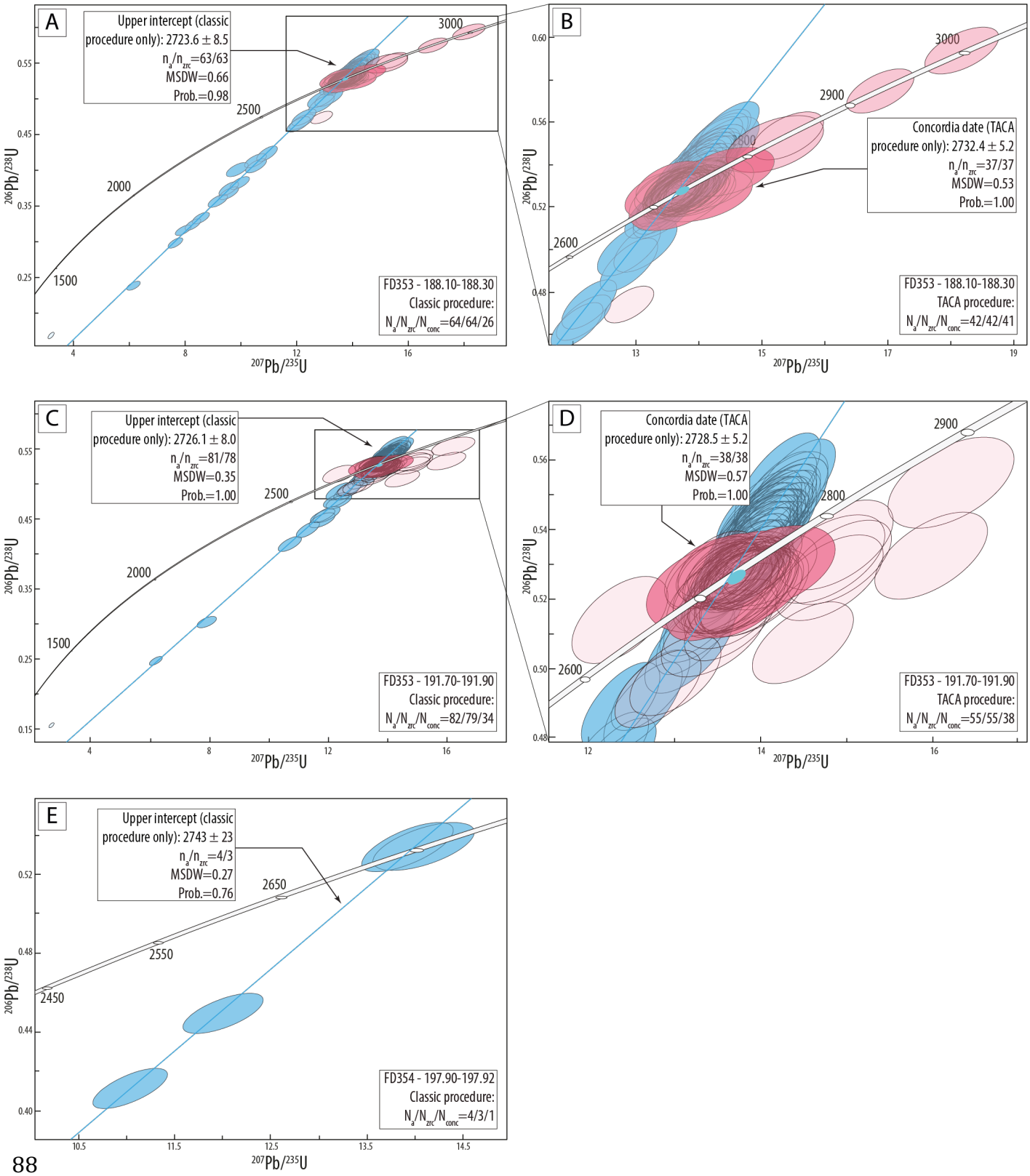

Supplementary Figure 4. Geochronological diagrams for samples collected in the Carajás Formation to the south of the basin. All the diagrams were generated using Isoplot/Ex 3.00 (Ludwig, 2012). Error ellipses are depicted at the 2σ level. N_a: number of analyses; N_{zrc}: number of zircon grains; N_{conc}: number of concordant zircon grains.

MSWD: Mean Square Weighted Deviate (given for both concordance and equivalence when referring to a concordia date); Prob.: probability if fit of the regression (upper intercept date) or probability for concordance and equivalence (concordia date). See Supplementary Fig. 3 for ellipse color legend. (**A**) Sample FD353 188.10-188.30. All analyses from both subsets. (**B**) Sample FD353 188.10-188.30. Inset focused on TACA analyses. (**C**) Sample FD353 191.70-191.90. All analyses from both subsets. (**D**) Sample FD353 191.70-191.90. Inset focused on TACA analyses.(**E**) Sample FD354 197.90-197.92. All analyses.

Supplementary Table 4. Comparison of maximum depositional ages obtained from untreated and TACA zircon grains.

Sample	N_{zrc}	Probability of concordance ≥ 10%, decay constants errors included								
		Detection limits (%)				Maximum depositional age				
		$DL_{1(pL=0.5)}$	$DL_{1(pL=0.95)}$	$DL_{3(pL=0.5)}$	$DL_{3(pL=0.95)}$	Age	± (2σ)	n	MSWD	Probability
Drill core FD110										
FD110 - 359.00-359.35										
Upper intercept date						2727.8	7.9	86	0.63	0.997
Concordia age (TACA)	36	1.9	8.0	7.4	16.5	2719.6	5.6	35	0.47	1.00
Drill core FD353										
FD353 - 188.10-188.30										
Upper intercept date						2723.6	8.5	63	0.66	0.98
Concordia age (TACA)	41	1.7	7.0	6.5	14.6	2732.4	5.2	37	0.53	1.00
FD353 - 191.70-191.90										
Upper intercept date						2726.1	8.0	81	0.35	1.00
Concordia age (TACA)	38	1.8	7.6	7.0	15.7	2728.5	5.2	38	0.57	1.00
Drill core FD354										
FD354 - 197.90-197.92										
Upper intercept date						2743	23	4	0.27	0.76

TACA: Thermal Annealing – Chemical Abrasion; N_{zrc}: number of concordant zircon grain analyzed per sample; n: number of analyses used to calculate the maximum deposition age; DL: detection limit, calculated after Rossignol et al. (2016); DL_1: detection limit for at least one grain; DL_3: detection limit for at least three grains; $_{pL}$: probability level assigned to the detection limits; MSWD: mean square of weighted

deviates, for both concordance and equivalence for concordia ages. The probability given for the upper intercept age correspond to the probability of fit of the regression. The probability given for concordia ages are for both concordance and equivalence. To regress the data for upper intercept age calculation, the points are weighted proportionally to the inverse square of their errors ("model 1" regression in Isoplot; Ludwig, 2012).

101

102 *2.3. Discussion*

103 Under the same chemical abrasion settings, different samples have markedly different ratios
104 of zircon grains passing the dissolution step. Although based on a limited number of rock
105 samples, the present study shows that half of grains survived the TACA treatment in one
106 sample (FD110 359.00-359.35) while nearly all of those picked up in another sample (FD353
107 191.70-191.90) survived the same treatment, raising two issues for the analysis of detrital
108 zircon grains. Firstly, there is a risk to lose a sample by dissolving all its grains, and this requires
109 a special care to define chemical abrasion settings (Huyskens et al., 2016; Widmann et al.,
110 2019). Secondly, differences in survival rate could bias a U-Pb detrital zircon datasets by
111 specifically wiping out one population while keeping others intact. This potential issue is likely
112 counterbalanced by the fact that grains not surviving TACA treatment are probably those
113 corresponding to the most discordant ones (Huyskens et al., 2016; Widmann et al., 2019). This
114 issue nonetheless deserves further investigations to ensure that no bias is introduced by TACA
115 treatment on detrital zircon populations. A safe strategy, but time consuming, would consist
116 in dating different subsets of untreated and TACA grains processed under different chemical
117 abrasion intensities in terms of HF concentration or leaching duration and temperature
118 (Huyskens et al., 2016; Widmann et al., 2019) to avoid sample loss and control potential bias
119 for provenance studies.

120 The TACA procedure significantly improved the concordance of analyzed zircon: in the
121 present study, only 50% of the analyses performed on untreated grains are concordant, while

76% of the TACA analyses are concordant (Supplementary Fig. 5). These results show the overall efficiency of TACA treatment to remove discordant parts of the grains. A higher ratio of concordant analyses after TACA treatment is in agreement with previous results obtained with thermal annealing alone (Solari et al., 2015) or by coupled thermal annealing and chemical abrasion (Crowley et al., 2014; von Quadt et al., 2014). In one sample (FD110 359.00-359.35), however, the TACA treatment did not improve the concordance ratio following the concordance criteria used in this study (Supplementary Fig. 5). Nonetheless, ca. 85% of the TACA analyses of FD110 359.00-359.35 have a probability of concordance higher than 1%, while this is the case for only 70% of the analyses without TACA treatment (Supplementary Fig. 5), showing the overall improvement of concordance by the TACA procedure. Such a limited to neutral effect of TACA to the concordance ratio has already been reported by other studies (Watts et al., 2016) and highlights different responses of zircon populations to TACA treatment. In the present study, however, the three samples contain essentially the same zircon population (see below). Inter-sample variations are likely related to a statistical bias, because not enough analyses have been performed, as suggested by the rather high detection limits obtained in this study (Supplementary Table 4).

Comparing maximum depositional ages calculated from classic and TACA analyses shows that identical results, within uncertainties, are obtained for a given sample (Supplementary Table 4). Thus, TACA treatment represents an efficient way to maximize the output of detrital zircon studies by increasing the number of concordant analyses at minimal costs, even if, in some cases, the concordance rate is not significantly improved.

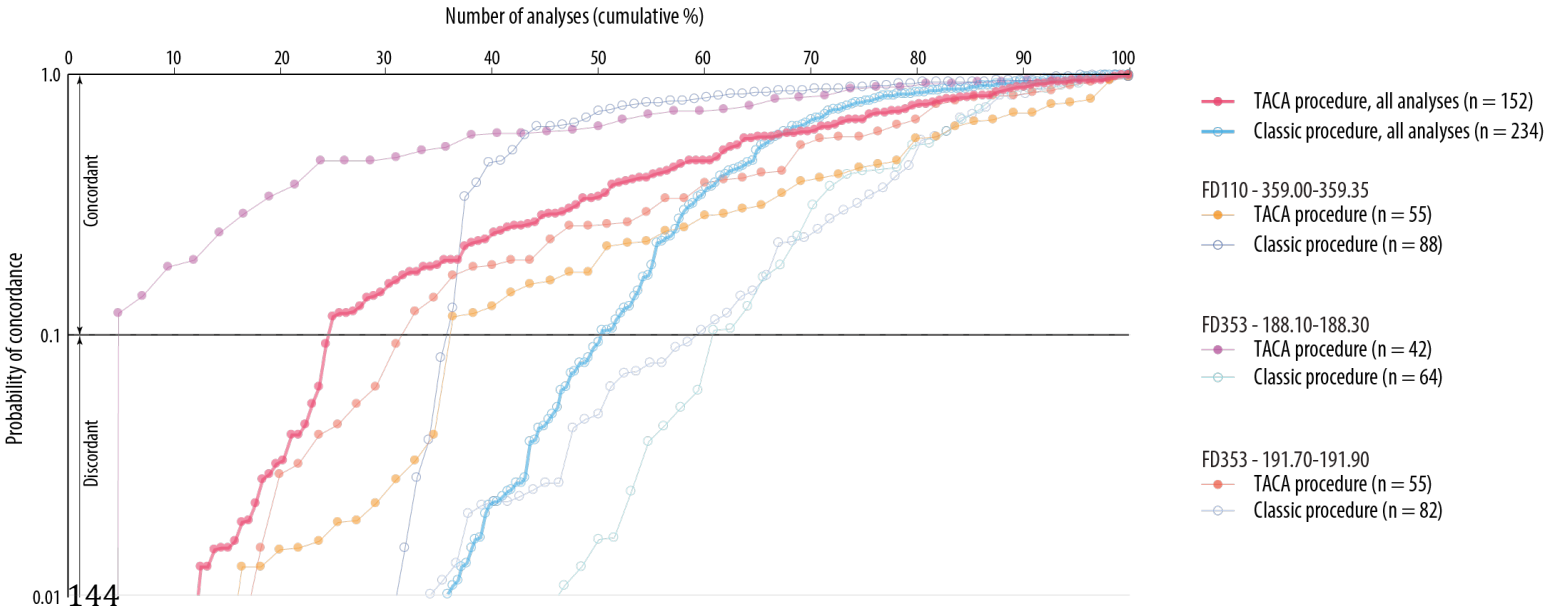

Supplementary Figure 5. Comparison of concordance with and without thermal annealing – chemical abrasion treatment. Decay constant errors are included in the calculation of probabilities of concordance. The cut-off value to define concordant analyses is 0.1. Analyses with a probability of concordance < 0.01 are not shown.

5.2. Complementary geochronological results for the Igarapé Bahia Group and Águas Claras Formation

Cathodoluminescence (CL) images of representative grains from the Igarapé Bahia Group and Águas Claras Formation (Supplementary Fig. 1) are presented in Supplementary Fig. 6. Complementary diagrams for the Igarapé Bahia Group, with all analyses (including the discordant ones), are presented in Supplementary Fig. 7.

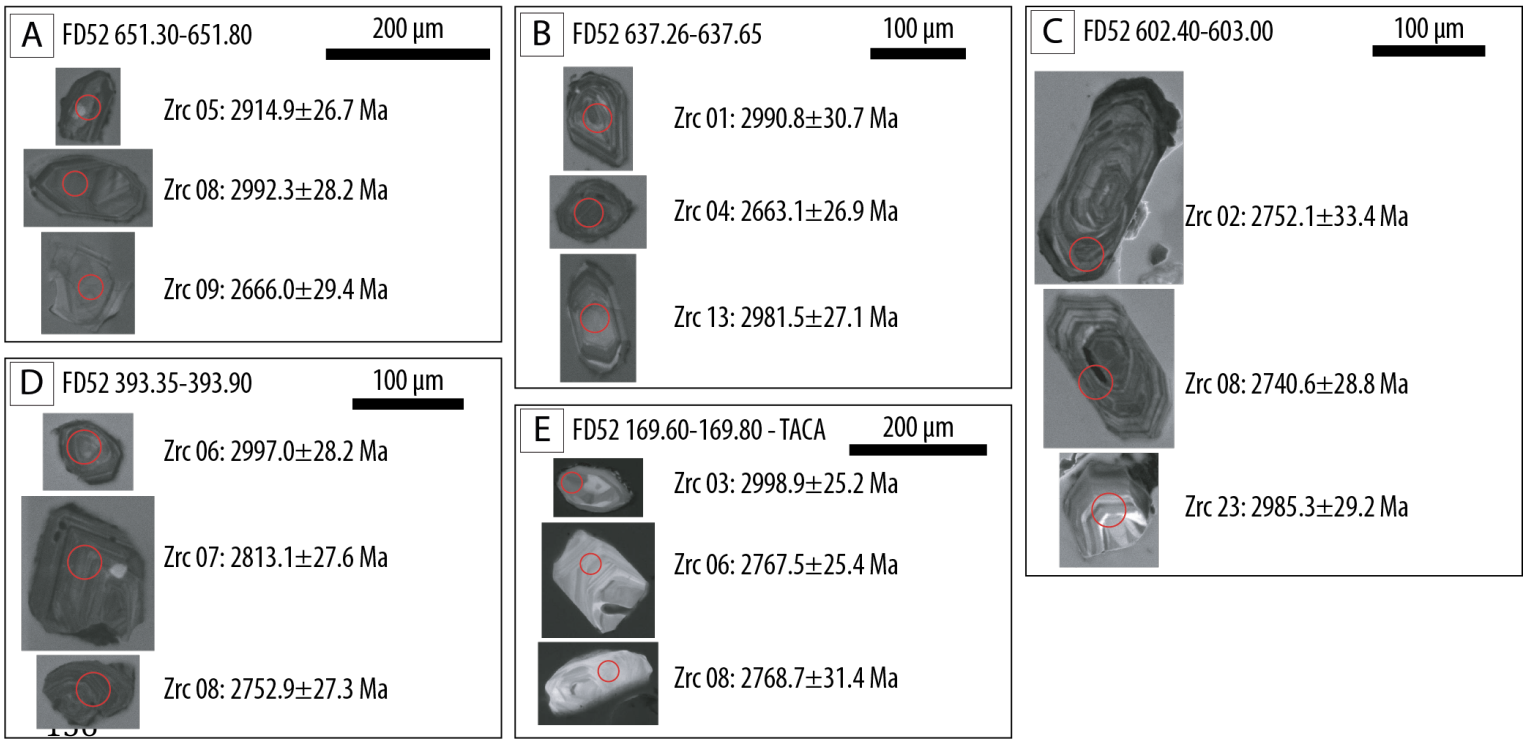

Supplementary Figure 6. Cathodoluminescence images of representative zircon grains of the Igarapé Bahia Group and the Águas Claras Formation. Red circles indicate the location of analyses. Uncertainties are given at the 2σ level. (**A**) Sample FD52 651.30-651.80. Igarapé Bahia Group. (**B**) Sample FD52 637.26-637.65. Igarapé Bahia Group. (**C**) Sample FD52 602.40-603.00. Igarapé Bahia Group. (**D**) Sample FD52 393.35-393.90. Igarapé Bahia Group. (**E**) Sample FD52 169.60-169.80. Águas Claras Formation.

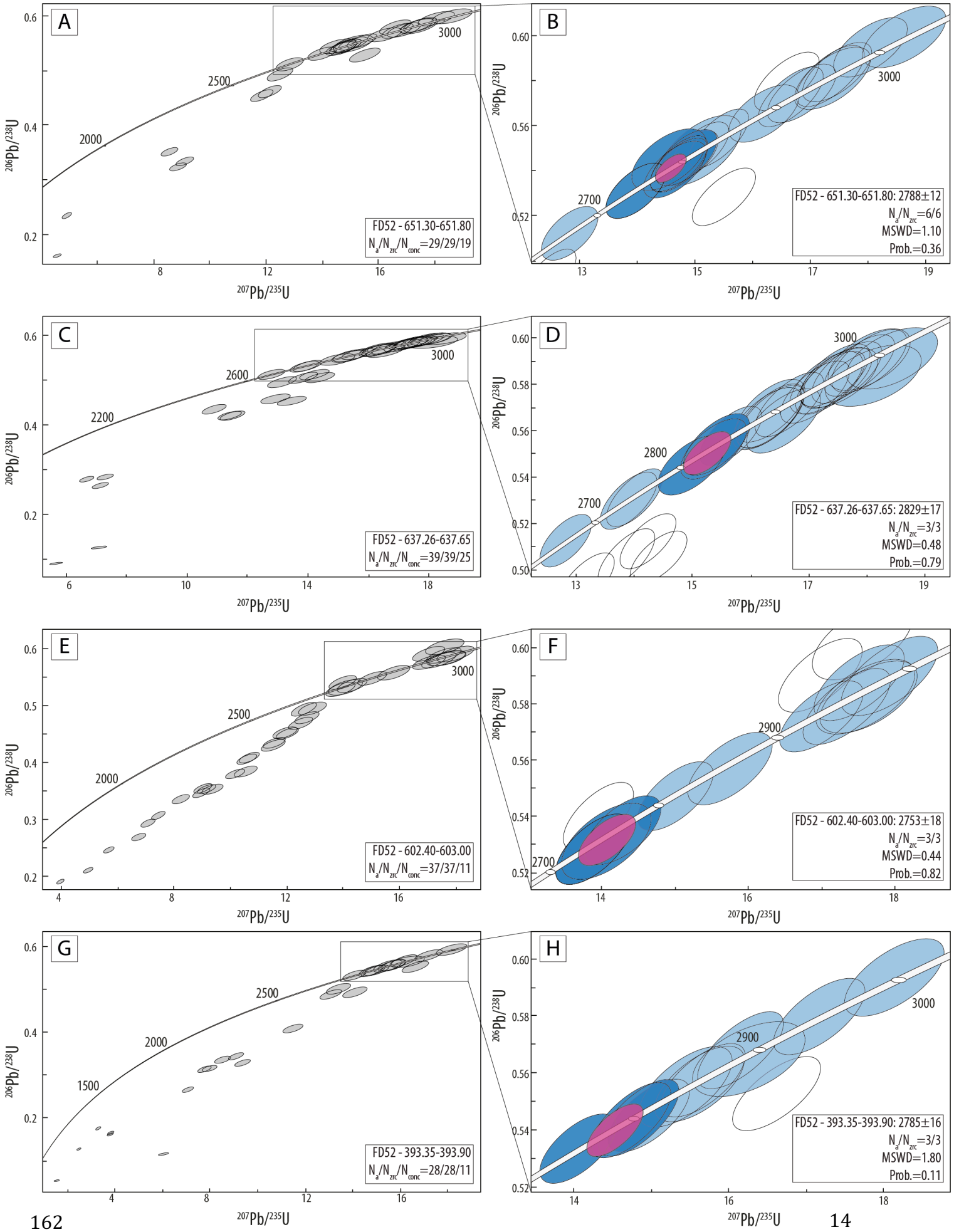
A
FD52 - 651.30-651.80
N_a/N_zrc/N_conc=29/29/19
B
FD52 - 651.30-651.80: 2788±12
N_a/N_zrc=6/6
MSWD=1.10
Prob.=0.36
C
FD52 - 637.26-637.65
N_a/N_zrc/N_conc=39/39/25
D
FD52 - 637.26-637.65: 2829±17
N_a/N_zrc=3/3
MSWD=0.48
Prob.=0.79
E
FD52 - 602.40-603.00
N_a/N_zrc/N_conc=37/37/11
F
FD52 - 602.40-603.00: 2753±18
N_a/N_zrc=3/3
MSWD=0.44
Prob.=0.82
G
FD52 - 393.35-393.90
N_a/N_zrc/N_conc=28/28/11
H
FD52 - 393.35-393.90: 2785±16
N_a/N_zrc=3/3
MSWD=1.80
Prob.=0.11
206Pb/238U
207Pb/235U

Supplementary Figure 7. Geochronological diagrams for the Igarapé Bahia Group. All the diagrams were generated using Isoplot/Ex 3.00 (Ludwig, 2012). Error ellipses are depicted at the 2σ level. In diagrams of the left columns, all data are plotted and are depicted in grey. On the right columns, concordant ellipses are depicted in pale blue, concordant ellipses used to calculate the maximum depositional age are depicted in dark blue and the weighted mean error ellipse (concordia date) of the youngest cluster of concordant grains is depicted in pink. Discordant (probability of concordance < 10%) analyses are depicted by open ellipses. N_a: number of analyses performed for each sample; N_{zrc}: number of analyzed grains; N_{conc}: number of concordant grains. MSWD: Mean Square Weighted Deviate for concordance and equivalence; Prob.: probability for concordance and equivalence. (**A**) Sample FD52 651.30-651.80. (**B**) Focus on the youngest concordant cluster of the sample FD52 651.30-651.80. (**C**) Sample FD52 637.26-637.65. (**D**) Focus on the youngest concordant cluster of the sample FD52 637.26-637.65. (**E**) Sample FD52 602.40-603.00. (**F**) Focus on the youngest concordant cluster of the sample FD52 602.40-603.00. (**G**) Sample FD52 393.35-393.90. (**H**) Focus on the youngest concordant cluster of the sample FD52 393.35-393.90.

The sample *FD52 169.60-169.*80 was collected ca. 2.5 m below a mafic dyke intruding the Águas Claras Formation (Supplementary Fig. 1) and corresponds to a conglomerate with angular volcaniclasts (G4 facies; Supplementary Table 2). This conglomerate is either a blocky peperite or a volcaniclastic rock deposited by debris flow. The sample yielded a fair amount of zircon grains characterized by diversified shapes, from euhedral to sub-rounded, various colors and sizes. Most of the grains are sub-angular and exhibit a pink to reddish color. Euhedral grains are slightly elongated with translucent, pinkish or reddish colors and sometimes contain inclusions. Other rounded to sub-rounded grains display various reddish or brownish grains colors. One hundred grains were selected for TACA treatment. About 80 grains were recovered after the treatment, and most of the grains (ca. 65) display an orange color and a strongly etched texture. These grains are non-luminescent in CL and attempts to date them only gave discordant dates indicating that the TACA treatment has not been

efficient on them. About 15 out of the 80 recovered grains became translucent and spotless, among which nine are concordant. This yields very high detection limits of 5.4% for the $DL_{1(pL=0.5)}$ and 55.5% for the $DL_{3(pL=0.95)}$. Grains that became translucent and spotless after the TACA treatment have a bright CL intensity and revealed well-defined oscillatory to faint and broad zoning (Supplementary Fig. 6) typical of magmatic zircon. Such origin is corroborated by the Th/U ratio of the grains, ranging from 0.11 to 1.11.

Four grains define the youngest cluster of analyses and give a concordia date of 2756 ± 13 Ma (MSWD = 0.87, probability = 0.53; Supplementary Fig. 8). Three other concordant grains are slightly older than the youngest cluster, with dates of 2805 ± 26 Ma to 2831 ± 24 Ma. Two other concordant grains give older Mesoarchean dates of 2928 ± 25 Ma and 2999 ± 25 Ma.

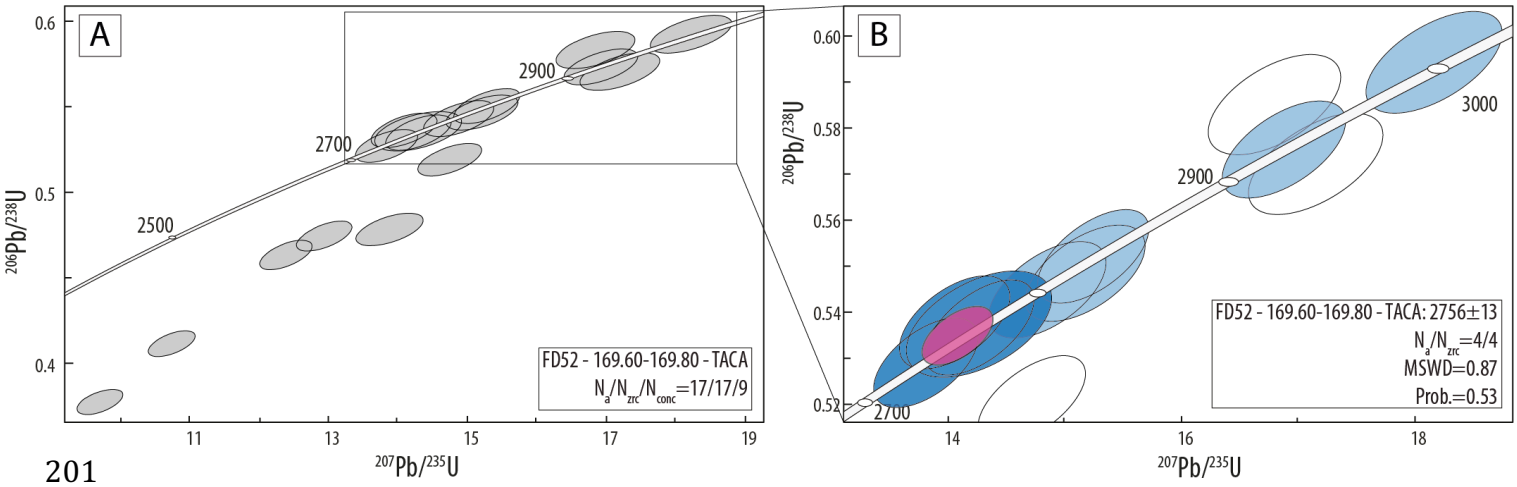

Supplementary Figure 8. Geochronological diagrams for the Águas Claras Formation. TACA: Thermal Annealing – Chemical Abrasion. (**A**) Sample FD52 169.60-169.80. (**B**) Focus on the youngest concordant cluster of the sample FD52 169.60-169.80.

Regarding the date given by the youngest cluster of analyses (2756 ± 13 Ma), two different interpretations can be proposed according to the nature of the conglomerate (debris flow

208 conglomerate *versus* blocky peperite). If the volcaniclastic rock where the zircon grains have
209 been picked up is a debris flow conglomerate, this date corresponds to a maximum
210 depositional age. If the conglomerate is a blocky peperite, the zircon grains that define the
211 youngest cluster are epicrysts or xenocrysts, or both, but are not autocrysts or antecrysts
212 (Rossignol et al., 2019), because it is older than the maximum depositional age of the
213 underlying Igarapé Bahia Group. Thus, in both cases (debris flow conglomerate or blocky
214 peperite), the date of 2756 ± 13 Ma corresponds to the maximum depositional age of the
215 Águas Claras Formation. This age is identical to the one of 2763 $\pm$ 32 Ma, based on only one
216 grain, proposed by Melo et al. (2019). Unfortunately, as being older than the maximum
217 depositional age of the Igarapé Bahia Group, this age does not provide a useful time
218 constraint. Another volcaniclastic sample from the Águas Claras Formation yielded a zircon U-
219 Pb date of 2681 ± 5 Ma and was interpreted as a depositional age by Trendall et al. (1998).
220 This date is identical, within uncertainties, to the maximum depositional age of the Igarapé
221 Bahia Group (2684 ± 10 Ma). Because there is no evidence for a volcanic activity coeval to the
222 deposition of the Águas Claras Formation, and because it is identical to the maximum
223 depositional age of the Igarapé Bahia Group, we reinterpret the 2681 ± 5 Ma date of Trendall
224 et al. (1998) as a maximum depositional age.

225 Our observations of the Águas Claras Formation clearly indicate that fluid circulation
226 imprinted this formation, as shown by the hydrothermal breccias between 270 m and 217 m
227 (Supplementary Fig. 1). The age of fluid circulation is a matter of debate: Melo et al. (2019)
228 suggested it occurred at ca. 2575 Ma, while Dreher et al. (2008) argued that the 2575 Ma fluid
229 circulation overprinted only the Igarapé Bahia Group and left the Águas Claras Formation
230 unaffected. In the drill core FD52, the hydrothermal breccias are related to a sill intrusion, so
231 that the age of fluid circulation is probably close to the one of the sill. The age of this sill is

unknown, but could correspond to one of the several generations of dykes that intruded the whole area at ca. 1880 Ma, 535 Ma and 200 Ma (Teixeira et al., 2019). None of these ages of dyke emplacement provide new constraint on the age of the Águas Claras Formation. Consequently, the only reliable age bounds for the Águas Claras Formation give a large time interval, between 2681 ± 5 Ma (Trendall et al., 1998) and 1880 ± 2 Ma (Machado et al., 1991).

References

Crowley, Q., Heron, K., Riggs, N., Kamber, B., Chew, D., McConnell, B., Benn, K., 2014. Chemical Abrasion Applied to LA-ICP-MS U–Pb Zircon Geochronology. Minerals 4, 503–518. https://doi.org/10.3390/min4020503

Dreher, A.M., Xavier, R.P., Taylor, B.E., Martini, S.L., 2008. New geologic, fluid inclusion and stable isotope studies on the controversial Igarapé Bahia Cu-Au deposit, Carajás Province, Brazil. Miner. Depos. 43, 161–184. https://doi.org/10.1007/s00126-007-0150-6

Horstwood, M.S.A., Kosler, J., Gehrels, G.E., Jackson, S.E., McLean, N.M., Paton, C., Pearson, N.J., Sircombe, K., Sylvester, P., Vermeesch, P., Bowring, J.F., Condon, D.J., Schoene, B., 2016. Community-Derived Standards for LA-ICP-MS U-(Th-) Pb Geochronology – Uncertainty Propagation, Age Interpretation and Data Reporting. Geostand. Newsl. 40, 311–332. https://doi.org/10.1111/j.1751-908X.2016.00379.x

Huyskens, M.H., Zink, S., Amelin, Y., 2016. Evaluation of temperature-time conditions for the chemical abrasion treatment of single zircons for U-Pb geochronology. Chem. Geol. 438, 25–35. https://doi.org/10.1016/j.chemgeo.2016.05.013

Jackson, S.E., Pearson, N.J., Griffin, W.L., Belousova, E.A., 2004. The application of laser ablation-inductively coupled plasma-mass spectrometry to in situ U–Pb zircon

geochronology. Chem. Geol. 211, 47–69. https://doi.org/10.1016/j.chemgeo.2004.06.017

Košler, J., Sláma, J., Belousova, E., Corfu, F., Gehrels, G.E., Gerdes, A., Horstwood, M.S.A., Sircombe, K.N., Sylvester, P.J., Tiepolo, M., Whitehouse, M.J., Woodhead, J.D., 2013. U-Pb Detrital Zircon Analysis - Results of an Inter-laboratory Comparison. Geostand. Geoanalytical Res. 37, 243–259. https://doi.org/10.1111/j.1751-908X.2013.00245.x

Košler, J., Sylvester, P.J., 2003. Present Trends and the Future of Zircon in Geochronology: Laser Ablation ICPMS, in: Hanchar, J.M., Hoskin, P.W.O. (Eds.), Zircon. Mineralogical Society of America and Geochemical Society, Washington, DC, United States, pp. 243–275.

Ludwig, K.R., 2012. User's Manual for a geochronological toolkit for Microsoft Excel. Berkeley Geochronological Cent. 75.

Machado, N., Lindenmayer, Z., Krogh, T.E., Lindenmayer, D., 1991. U-Pb geochronology of Archean magmatism and basement reactivation in the Carajás area, Amazon shield, Brazil. Precambrian Res. 49, 329–354. https://doi.org/10.1016/0301-9268(91)90040-H

Melo, G.H.C., Monteiro, L.V.S., Xavier, R.P., Moreto, C.P.N., Arquaz, R.M., Silva, M.A.D., 2019. Evolution of the Igarapé Bahia Cu-Au deposit, Carajás Province (Brazil): Early syngenetic chalcopyrite overprinted by IOCG mineralization. Ore Geol. Rev. 111, 102993. https://doi.org/10.1016/j.oregeorev.2019.102993

Moreto, C.P.N., Monteiro, L.V.S., Xavier, R.P., Creaser, R.A., DuFrane, S.A., Tassinari, C.C.G., Sato, K., Kemp, A.I.S., Amaral, W.S., 2015. Neoarchean and paleoproterozoic iron oxide-copper-gold events at the sossego deposit, Carajás Province, Brazil: Re-Os and U-Pb geochronological evidence. Econ. Geol. 110, 809–835. https://doi.org/10.2113/econgeo.110.3.809

279 Pidgeon, R.T., MacAmbira, M.J.B., Lafon, J.M., 2000. Th-U-Pb isotopic systems and internal
280 structures of complex zircons from an enderbite from the Pium Complex, Carajas
281 Province, Brazil: Evidence for the ages of granulite facies metamorphism and the
282 protolith of the enderbite. Chem. Geol. 166, 159–171. https://doi.org/10.1016/S0009-
283 2541(99)00190-4
284 Rossignol, C., Bourquin, S., Poujol, M., Hallot, E., Dabard, M.-P., Nalpas, T., 2016. The
285 volcaniclastic series from the Luang Prabang Basin, Laos: A witness of a triassic magmatic
286 arc? J. Asian Earth Sci. 120. https://doi.org/10.1016/j.jseaes.2016.02.001
287 Rossignol, C., Hallot, E., Bourquin, S., Poujol, M., Jolivet, M., Pellenard, P., Ducassou, C., Nalpas,
288 T., Heilbronn, G., Yu, J., Dabard, M.-P., 2019. Using volcaniclastic rocks to constrain
289 sedimentation ages: To what extent are volcanism and sedimentation synchronous?
290 Sediment. Geol. 381, 46–64. https://doi.org/10.1016/J.SEDGEO.2018.12.010
291 Santos, M.M., Lana, C., Scholz, R., Buick, I., Schmitz, M.D., Kamo, S.L., Gerdes, A., Corfu, F.,
292 Tapster, S., Lancaster, P., Storey, C.D., Basei, M.A.S., Tohver, E., Alkmim, A.R., Nalini, H.,
293 Krambrock, K., Fantini, C., Wiedenbeck, M., 2017. A New Appraisal of Sri Lankan BB Zircon
294 as a Reference Material for LA-ICP-MS U-Pb Geochronology and Lu-Hf Isotope Tracing.
295 Geostand. Geoanalytical Res. 41, 335–358. https://doi.org/10.1111/ggr.12167
296 Sircombe, K.N., Stern, R.A., 2002. An investigation of artificial biasing in detrital zircon U-Pb
297 geochronology due to magnetic separation in sample preparation. Geochim. Cosmochim.
298 Acta 66, 2379–2397.
299 Sláma, J., Košler, J., Condon, D.J., Crowley, J.L., Gerdes, A., Hanchar, J.M., Horstwood, M.S.A.,
300 Morris, G.A., Nasdala, L., Norberg, N., Schaltegger, U., Schoene, B., Tubrett, M.N.,
301 Whitehouse, M.J., 2008. Plešovice zircon — A new natural reference material for U–Pb
302 and Hf isotopic microanalysis. Chem. Geol. 249, 1–35.

https://doi.org/10.1016/j.chemgeo.2007.11.005

Solari, L.A., Ortega-Obregón, C., Bernal, J.P., 2015. U-Pb zircon geochronology by LAICPMS combined with thermal annealing: Achievements in precision and accuracy on dating standard and unknown samples. Chem. Geol. 414, 109–123. https://doi.org/10.1016/j.chemgeo.2015.09.008

Teixeira, W., Hamilton, M.A., Girardi, V.A.V., Faleiros, F.M., Ernst, R.E., 2019. U-Pb baddeleyite ages of key dyke swarms in the Amazonian Craton (Carajás/Rio Maria and Rio Apa areas): Tectonic implications for events at 1880, 1110 Ma, 535 Ma and 200 Ma. Precambrian Res. 329, 138–155. https://doi.org/10.1016/j.precamres.2018.02.008

Trendall, A.F., Basei, M.A.S., De Laeter, J.R., Nelson, D.R., 1998. SHRIMP zircon U-Pb constraints on the age of the Carajas formation, Grao Para Group, Amazon Craton. J. South Am. Earth Sci. 11, 265–277. https://doi.org/10.1016/S0895-9811(98)00015-7

van Achterbergh, E., Ryan, C.G., Griffin, W.L., 2004. GLITTER! User's manual.

von Quadt, A., Gallhofer, D., Guillong, M., Peytcheva, I., Waelle, M., Sakata, S., 2014. U-Pb dating of CA/non-CA treated zircons obtained by LA-ICP-MS and CA-TIMS techniques: Impact for their geological interpretation. J. Anal. At. Spectrom. 29, 1618–1629. https://doi.org/10.1039/C4JA00102H

Watts, K.E., Coble, M.A., Vazquez, J.A., Henry, C.D., Colgan, J.P., John, D.A., 2016. Chemical abrasion-SIMS (CA-SIMS) U-Pb dating of zircon from the late Eocene Caetano caldera, Nevada. Chem. Geol. 439, 139–151. https://doi.org/10.1016/j.chemgeo.2016.06.013

Widmann, P., Davies, J.H.F.L., Schaltegger, U., 2019. Calibrating chemical abrasion: Its effects on zircon crystal structure, chemical composition and U–Pb age. Chem. Geol. 511, 1–10. https://doi.org/10.1016/j.chemgeo.2019.02.026